Double Ionization of Quaterrylene ($C_{40}H_{20}$) in Water-Ice at 20 K with Ly_α (121.6 nm) Radiation

Murthy S. Gudipati*,†,‡ and Louis J. Allamandola†,§

NASA Ames Research Center, Mail Stop 245-6, Moffett Field, California 94035, and Institute for Physical Sciences and Technology, University of Maryland, College Park, Maryland 20742

Received: March 7, 2006; In Final Form: May 16, 2006

Polycyclic aromatic hydrocarbon (PAH) molecules undergo facile ionization in cryogenic water-ices resulting in near quantitative conversions of neutral molecules to the corresponding singly charged radical cations. Here we report, for the first time, the production and stabilization of a doubly ionized, closed shell PAH in water-ice. The large PAH quaterrylene (QTR, $C_{40}H_{20}$) is readily photoionized and stabilized as QTR^{2+} in a water-ice matrix at 20 K. The kinetic analysis of photolysis shows that the QTR^{2+} is formed at the expense of QTR^+, not directly from QTR. The long-axis polarized S_1-S_0 ($1^1B_{3u} \leftarrow 1^1A_g$) transition for QTR^{2+} falls at 1.59 eV (782 nm). TD-DFT calculations at the B3LYP level predict that this transition falls at 1.85 eV (670 nm) for free gas-phase QTR^{2+}, within the 0.3 eV uncertainty associated with these calculations. This red shift of 0.26 eV is quite similar to the 0.24 eV red shift between the TD-DFT computational prediction for the lowest energy transition for QTR^+ (1.68 eV) and its value in a water matrix (1.44 eV). These results suggest that multiple photoionization of such large PAHs in water-ice can be an efficient process in general.

Introduction

The chemistry and physics of low-temperature water-ices and impurities trapped within are undergoing a revival of interest due to recent advances in astrophysics and atmospheric science. Water-rich, mixed molecular ices are common throughout interstellar molecular clouds,[1] the Solar System,[2,3] and atmospheric aerosols.[4] Laboratory analogue experiments have shown vacuum ultraviolet (VUV) irradiation and particle bombardment of water dominated mixed molecular ices containing impurities such as CH_3OH, NH_3, CO and PAHs (polycyclic aromatic hydrocarbons) produce complex organic species, including important biogenic molecules such as amino acids and functionalized PAHs which may have played a role in the origin of life.[5−10]

In an attempt to understand the fundamental processes that occur during VUV photolysis of water dominated mixed molecular ices containing PAHs, several counterintuitive phenomena were recently discovered. PAHs embedded in cryogenic water-ice are easily and efficiently ionized (>80%, i.e., near quantitative ion yields) to the cation form by VUV photons;[11,12] PAH ionization energy is lowered by up to 2 eV compared to that in the gas phase,[13] in agreement with recent theoretical predictions;[14,15] and PAH cations are stabilized to temperatures as high as 120 K.[16] Here we report, for the first time, that closed-shell PAH dications can also be produced and stabilized in water-ice.

The results presented here show that the PAH quaterrylene (QTR), when trapped in water-ice at a low temperature, can be doubly ionized to the QTR dication (QTR^{2+}) through a sequential ionization process, QTR to QTR^+ to QTR^{2+}, with Ly_α photons (121.6 nm, 10.2 eV). Up to now, multiple ionization of aromatic molecules is known only in the gas phase and detection is typically via mass spectrometry.[17,18] Direct double photoionization of aromatic molecules needs high-energy photons, as illustrated in the case of naphthalene. The first ionization threshold of naphthalene is at 8.12 eV, whereas double photoionization requires photons with energies greater than 21 eV.[19]

Other recent work on energetic processing of water-ices includes the study of molecular dissociation through photolysis and radiolysis,[20,21] and the chemistry of anthropogenic aromatic pollutants in arctic ice.[22] Electron bombardment of water-ice surfaces has recently been shown to produce protons and hydrogen molecular cations as a result of dissociative ionization of water molecules on the surface.[23] To the best of our knowledge, there are no reports of sequential double ionization of aromatic molecules with photons as low in energy as Ly_α.

Experimental Section

The experimental setup, consisting of a cryogenic sample holder, a spectrograph and detector has been described elsewhere.[13,24] For the present studies, the QTR containing water-ice was deposited onto a LiF window and a 100 W quartz−tungsten halogen lamp was used to record single beam transmission spectra. Photoionization of QTR was carried out using a microwave-powered, flowing hydrogen-discharge lamp which produces Ly_α radiation at 121.6 nm and a roughly 20 nm wide band of molecular hydrogen emission lines centered near 160 nm, with a flux of approximately 2×10^{15} photons/s.

QTR (molecular structure shown in Figure 1) was obtained from Dr. W. Schmidt (PAH Forschungs Institut, Greifenberg, Germany) and used without further purification. High-purity deionized water (18 MΩ) was deposited at an approximate rate of 0.02 mmol h^{-1} onto a LiF cryogenic optical window kept at 30 K. Quaterrylene vapor was simultaneously deposited onto

* Corresponding author. E-mail: gudipati@glue.umd.edu, mgudipati@arc.nasa.gov.
† NASA Ames Research Center.
‡ IPST, University of Maryland.
§ E-mail: louis.j.allamandola@nasa.gov.

10.1021/jp061416n CCC: $33.50
Published on Web 06/27/2006

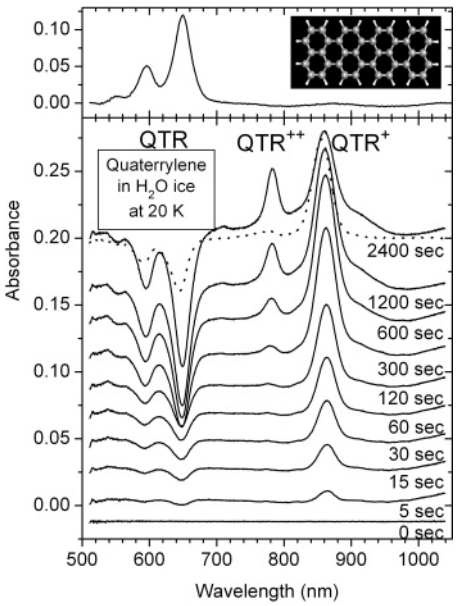

Figure 1. Electronic absorption spectra of quaterrylene (QTR) and its mono- and dications in a water matrix at 20 K as a function of VUV photolysis time with the hydrogen discharge lamp. This lamp emits 121.6 nm (Ly_α) radiation and a broad emission centered at 160 nm. The absorption spectrum of a freshly deposited neutral quaterrylene (QTR)/$H_2O \sim 1/500$) sample is shown in the upper frame where neutral QTR is responsible for the vibronic band series starting at 650 nm. The lower frame shows the spectral changes that occur in this ice when it is photolyzed. The negative absorbance bands correspond to the loss of neutral QTR whereas the positive bands arise from the photoproducts. The spectra of the corresponding radical cation (QTR^+) at 860 nm, evident immediately upon photolysis, and the absorption we assign to the closed-shell dication (QTR^{2+}) at 782 nm can clearly be seen. The 782 nm band has an induction period and then grows steadily with prolonged irradiation, eventually comparable to the 860 nm QTR^+ absorption band. Photolysis times are given below each spectrum. Close to 80% of the neutral QTR is depleted during the 2400 s VUV photolysis. For comparison, the spectrum from a similar experiment that employed defocused 266 nm Nd:YAG laser photons (instead of Ly_α) to ionize the QTR in a water matrix after 2700 s photolysis, is shown as the dotted spectrum overlaid on the 2400 s spectrum. In this case no significant absorption arising from QTR^{2+} is seen at 782 nm. The energy of the 266 nm laser photons (4.66 eV) is sufficient only for the first ionization of QTR to QTR^+ in the water-ice, but not for the subsequent ionization to QTR^{2+}, which needs about 6 to 7 eV.

the cold window at a rate approximately 500 times slower, resulting in a dilution of 1:500. The QTR vapor was generated in a 1 cm inside-diameter, glass tube containing solid QTR and heated to 300 °C. This tube was attached to the cryogenic sample chamber and the opening positioned roughly 3 cm from the cold window. The QTR and water vapor streams were co-deposited for about 4 h, during which time transmission spectra were measured to monitor the optical depth of the absorption by QTR as well as the optical quality of the ice. Once an ice of sufficient thickness and QTR optical depth was formed, it was subsequently cooled to 20 K at a rate of 1 K/min. We have found that the cryogenic water matrices prepared in this way have very good optical properties, showing no haze or cracks and possess an optical quality comparable to rare-gas matrices.[12] Under these experimental conditions water deposited on substrates held at lower temperatures (20 K) are optically hazy, whereas the optical quality improves when the water matrices are formed on a window at higher temperature. To keep the substrate temperature as low as possible during deposition, a compromise was made to maintain the window at 30 K during deposition.

Single-beam transmission spectra were recorded and stored in the computer after each deposition or photolysis period. These transmission spectra were then converted to absorption spectra by using the single-beam transmission spectrum before photolysis as the reference. Using this procedure, negative bands indicated depletion of the molecular species whereas positive bands result from creation of new molecular species. To simultaneously monitor the absorption by both the neutral and radical cation forms of QTR within the same frame of the spectrum, the limits of the 0.25 m spectrometer were set at 510 and 1040 nm.

Results and Discussion

Section 1: Identification of QTR^{2+}. Throughout the following we use water-ice and water matrix interchangeably to represent the cryogenic H_2O solid, in either the amorphous or crystalline phases as specified. The absorption spectrum of a QTR/H_2O ($\sim$1/500) ice at 20 K, prepared by 4 h of co-deposition of QTR and H_2O vapor onto the LiF window, is shown in the top-frame of Figure 1. This spectrum, which consists of a strong band peaking at 650 nm and two vibronic components at 595 and 550 nm, is due to the $S_1 \leftarrow S_0$ ($1^1B_{3u} \leftarrow 1^1A_g$) transition in QTR, which has an oscillator strength of 1.08.[25] The lower frame of Figure 1 shows the absorption spectra that were obtained at different VUV-photolysis doses, by taking the preirradiation spectrum (upper frame) as the reference. Between 0 and 600 s of photolysis, the simultaneous growth of a strong absorption band around 860 nm with a very weak satellite feature at 780 nm can be clearly seen. Both are due to the QTR radical cation (QTR^+) generated upon photoionization. These bands are assigned to the $D_2 \leftarrow D_0$ ($2^2B_{3g} \leftarrow 1^2A_u$) transition in QTR^+, which has an oscillator strength of 1.03.[25] The corresponding loss of the neutral parent QTR is about 50% after 600 s of photoionization. Upon prolonged photolysis, absorption overlapping the weak satellite feature at 780 nm grows more rapidly, whereas the dominant QTR^+ absorption band at 860 nm diminishes in intensity. After 2400 s of irradiation this becomes a strong band at 782 nm. We attribute this new band to QTR^{2+} for the reasons presented below. The integrated intensities of the neutral, monocation and dication QTR absorption bands at 650, 860, and 782 nm, respectively, are plotted versus photolysis time in Figure 2. Inspection of Figure 2 shows that there is an induction period before the onset of the appearance of the new band at 782 nm and that this onset and subsequent growth occurs at the expense of the growth rate of the 860 nm band of QTR^+. After about 600 s, the QTR^+ band growth rate clearly starts to diminish while the new feature continues to grow. During this same time the rate of loss of neutral QTR also slows. This shows that the carrier of the new feature is produced from QTR^+, not from neutral QTR directly. Only after enough population of QTR^+ is built up do we see the appearance of the 782 nm band, suggesting the photoionization of QTR^+ to QTR^{2+}. Thus, the delayed onset of the 782 nm absorption due to QTR^{2+} clearly rules out the direct double ionization of QTR neutral molecule. After 2400 s of VUV irradiation, close to 80% of the neutral QTR has become ionized.

Photokinetics. These photochemical reactions are modeled with Scheme 1 below. Reaction rates (k) are determined by manually changing the variable parameters in a manner similar to the procedure used to obtain the relative photoionization reaction rates of 4-methylpyrene in a water matrix.[12] The results are plotted as dashed lines in Figure 2. All the parameters are expressed in terms of k_2, which is determined to be 2.5×10^{-3} absorbance units per second ($k_1 = k_3 = 0.02k_2$, $k_{-2} = 0.45k_2$,

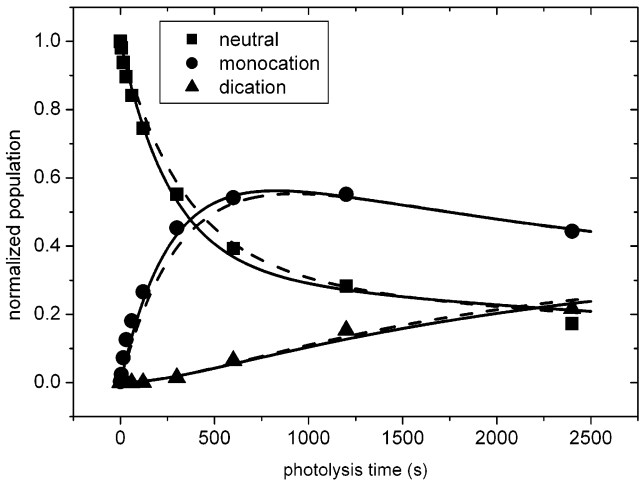

Figure 2. Curves showing the loss of QTR and the growth of QTR^+ and QTR^{2+} in a QTR/H_2O (1/500) matrix at 20 K as a function of in-situ photolysis time. For each neutral QTR point, the integrated absorbance of the 650 nm band is normalized to its initial value before photoionization. The ratio of the computed oscillator strengths for the bands of QTR (650 nm), QTR^+ (860 nm) and QTR^{2+} (782 nm), given in Table 1, are used to normalize the other points. Solid lines are best fits to the experimentally derived data shown as solid circles, squares, and triangles. The dashed lines are simulated using Scheme 1 described in the text.

SCHEME 1: VUV Photoinduced Reaction Scheme for QTR in a Water Matrix at 20 K[a]

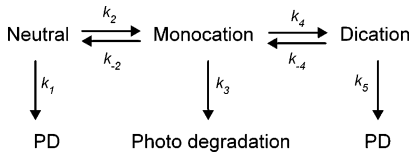

[a] PD indicates photodegradation products.

$k_4 = 0.1k_2$, $k_{-4} = 0.07k_2$, $k_5 = 0.01k_2$). The good agreement between the experimental data points and the dashed curves in Figure 2 support describing the photolytic production of the species responsible for the 782 nm band from QTR neutral as a predominantly two-step process involving singly ionized QTR^+ as the intermediate.

Host Photochemistry. Though the band-gap of ice is ill defined, work by several investigators[26] indicates that photoionization through ion-pair formation or autoionization of host water molecules in the ice also occurs at photon energies as low as 6.8 eV. Efficient ionization definitely occurs above 10 eV. Thus, irradiation with 121.6 nm photons can lead to mobile protons that can interact with the trapped QTR. Similarly, photodissociation of amorphous ices occurs 6.4 eV,[27] generating H and OH. Thus it is important to consider other possibilities due to the reactions of photoproducts of the host ice matrix, namely H, OH, H^+, and OH^- with QTR or QTR^+ as processes that may be responsible for the generation of a QTR^+ or a QTR^- related species which absorbs at 782 nm (Figure 1) during in-situ irradiation at 20 K. Our earlier studies showed that reactions that lead to the hydroxylation (addition of OH) to the PAH molecule naphthalene occurs at temperatures above 100 K.[12,16] Hence we consider only the possibility of reactions of QTR with H and H^+ below.

Up to now we have no evidence for such reactions between the imbedded small PAH molecules naphthalene, 4-methylpyrene, or pyrene occurring with host photoproducts in water ice at 20 K.[11−13,16] In all of these cases irradiation under identical conditions appears to result exclusively in the single ionization

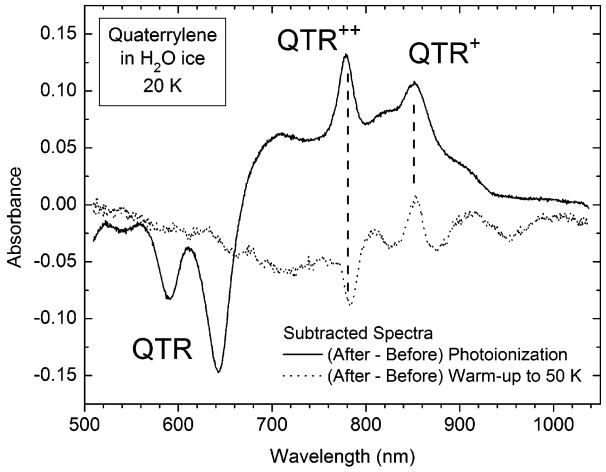

Figure 3. Results of careful warm-up experiments showing the generation of QTR^+ at the expense of the 782 nm absorption we assigned to QTR^{2+}. The solid spectrum is the difference spectrum (after irradiation − before irradiation). The dotted spectrum is the difference spectrum before and after a 20 K−50 K−20 K warm-up cycle (after warm-up − before warm-up). The corresponding changes in the bands are connected with dashed lines to guide the eye.

of the PAH to PAH^+. However, these reactions are considered here in light of the greater size of QTR. We exclude these reaction products as potential carriers of the 782 nm feature as described below. Keeping in mind that the carrier of the 782 nm absorption band is created at the expense of QTR^+, reactions that are pertinent to QTR^+ are only considered.

Under our experimental conditions in which Ly_α radiation (10.2 eV) is used, the maximum amount of energy that is available to the photoproducts H or H^+ is 3.4 eV because ion-pair and autoionization processes require 6.8 eV to occur in water ice.[26] Even if this energy is localized on one photoproduct, it is not sufficient to ionize QTR to QTR^+, a process that requires around 4.6 eV, or to doubly ionize QTR^+ to QTR^{2+}, a process that needs 6−7 eV to occur efficiently. Thus the role of secondary ionization reactions caused by ionized or dissociated host photoproducts through energy transfer can be neglected. The second possibility is the direct reaction of QTR^+ with the host photoproducts H or H^+ to produce the 782 nm band carriers. Such reactions may be possible, leading to the formation of $QTRH^+$ from QTR and $QTRH^{2+}$ from QTR^+, when H^+ reacts with the QTR or QTR^+, respectively. Similarly, it should be possible for H atoms to react with QTR to generate QTRH, and with QTR^+ to generate $QTRH^+$. We can rule out the possibility that a reaction product of neutral QTR with H or H^+ produces the 782 nm band because the behavior shown in Figure 2 and the kinetic analysis indicates that the species responsible for the 782 nm absorption is generated from QTR^+, not QTR. Protonation of QTR^+ seems less likely than protonation of neutral QTR due to Coulomb repulsion. This leaves $QTRH^+$, formed through H atom addition to QTR^+, as the possible alternative to QTR^{2+} as the carrier of the 782 nm band.

$QTRH^+$ is ruled out as the carrier of the 782 nm band as follows. After 2400 s of in-situ VUV photolysis, the QTR/H_2O ice was warmed to 50 K. As shown in Figure 3, the initial warm-up from 20 to 50 K resulted in slight depletion of the 782 nm band (assigned to QTR^{2+}) and growth of the 860 nm QTR^+ band. This is possible only if the species responsible for the 782 nm band absorption is something that readily reverts to QTR^+ in a water matrix at 50 K. It is highly unlikely that protonated QTR ($QTRH^+$) or a fragment of QTR^+ is the carrier of the 782 nm band as these species are not expected to

TABLE 1: Time Dependent, Density Functional Theory (TD-DFT) Energies (eV) for the Lowest Level Transitions of QTR, QTR^+, and QTR^{2+} Compared with the Values Measured in a Neon Matrix at 4 K and in Water-Ice at 20 K (Computed Oscillator Strengths (*f*) in Parentheses)

		experiment		theory[c]	
species	transition	Ne matrix[a]	H_2O matrix[b]	BLYP/6-31G* TD-DFT[a]	B3LYP/6-31G* TD-DFT[b]
neutral (QTR)	$1^1B_{3u} \leftarrow 1^1A_g$	2.04	1.91	1.67 (1.08)	1.87 (1.23)
monocation (QTR^+)	$2^2B_{3g} \leftarrow 1^2A_u$	1.48	1.44	1.62 (1.03)	1.68 (1.29)
dication (QTR^{2+})	$1^1B_{3u} \leftarrow 1^1A_g$		1.59		1.85 (1.4)

[a] From ref 25. [b] Present work, also from ref 13.

regenerate QTR^+ upon warm-up over this temperature domain in which the ice matrix does not undergo any major phase transitions.[28] On the other hand, we have found thermally promoted electron migration and electron−ion recombination over this temperature range in water ice, work which will be described elsewhere.

Theoretical Computations. To better understand the nature of the transition and the ionization energetics, time dependent-density functional theory (TD-DFT) computations were carried out on QTR^{2+}. The B3LYP method and 6-31G(d) basis sets using the GAUSSIAN03 program package[29] were used to determine the 0−0 transition energies for various ground-to-excited state transitions. Such calculations have already been reported for neutral and singly ionized QTR at the BLYP/6-31G* level.[29] The results of these calculations and the experimental values available are summarized in Table 1. The electronic states for the mono- and dications show similar matrix shifts (∼0.25 eV) between the gas-phase theory predictions and the values measured in a water matrix. All of the calculated values fall within 0.3 eV of the experimental values, the uncertainty normally associated with this level of calculation. Systematic studies show that indeed TD-DFT maintains uniform accuracy for open-shell (multiplets) and closed-shell (singlets) systems.[30] Interestingly, the matrix red shift in going from a Ne to H_2O matrix is smaller for QTR^+ (0.04 eV) than it is for neutral QTR (0.13 eV).

On the basis of the kinetic behavior shown in Figures 1 and 2, taken together with these calculations, we assign the absorption band at 782 nm to QTR^{2+}. These results suggest that the photoelectron is ejected from the site (cage) in which QTR^{2+} is generated and is subsequently stabilized at another "site" in the water matrix (cage-exit of the photoelectron). Given the greater electron affinity of H_2O matrix over Ne matrix, it is likely that electrons diffuse far more slowly and travel much smaller distances in a H_2O matrix compared to a Ne matrix.

The low first ionization energies of the neutral and singly charged QTR in H_2O matrix, combined with the ability of the H_2O matrix to stabilize the ionized molecules and the corresponding electrons, allows the significant single and double photoionization processes observed here with relatively mild photon energies (≤10.2 eV) and mild photon flux.

To have sequential photoionization of QTR with Ly_α photons, ionization threshold energies for both neutral QTR and QTR^+ below 10.2 eV are implied. To test this, the vertical ionization energies using the B3LYP method with 6-31G(d) basis sets were computed. For neutral QTR the computed ionization energy is 5.43 eV, in reasonably good agreement with the experimental value of 6.11 eV.[31] For the second ionization step, namely, QTR^+ to QTR^{2+}, the ionization energy is computed to be 8.3 eV. Thus, Ly_α radiation is sufficient to drive both steps of the sequential ionization processes.

Further support for the QTR^{2+} assignment is derived from the absence of the 782 nm absorption band when neutral QTR is irradiated in a water matrix with 266 nm laser photons under identical experimental conditions (dotted spectrum in Figure 1).[13] The energy of the 266 nm photons at 4.66 eV is sufficient only for the first ionization of QTR to QTR^+ in a water matrix.

Given the ability of a water matrix to lower the ionization energy of PAH molecules by about 2 eV,[12−14] it may be possible that even lower energy photons could doubly ionize such large PAHs in these matrices. As only single photoionization of QTR occurs in water matrices with 266 nm photons,[13] double ionization of QTR is expected to occur in such matrices at threshold photon energies of 6−7 eV. This range is deduced on the basis of the observed lowering of QTR ionization energy by ∼2 eV in water matrices and the computed second ionization threshold for gas-phase QTR to be ∼8−9 eV. When a hydrogen flow-discharge lamp is used, in addition to Ly_α photons at 121.6 nm (10.2 eV) due to atomic hydrogen, photons are also emitted from the molecular hydrogen around 160 nm. The energy of these lines centered around 7.75 eV, is sufficient to ionize QTR to QTR^+ and QTR^+ to QTR^{2+} in water ice (after taking lowering of the ionization energy of ∼2 eV in ice compared to that in the gas phase into account). Further work is underway to obtain threshold ionization energies for both QTR and QTR^+ in water-ices. We also plan to investigate if quaterrylene can be triply ionized to QTR^{3+} and stabilized in water-ices and extend these studies to PAHs of various sizes to understand how far these molecules can be ionized before they spontaneously break apart due to Coulomb repulsion.

Section 2: Comparison between QTR Photochemistry in H_2O and Neon Matrices. The absorption spectra of QTR, its monocation QTR^+, and its monoanion QTR^- have been measured by Halasinski et al. in Ne matrices.[25] The ions have been formed by in-situ irradiation of QTR isolated in a neon matrix in a manner similar to that described here. The detection of QTR^- in a neon matrix raises the possibility of its formation and stabilization in an H_2O matrix as well.

As one would expect, the vibronic bands of QTR trapped in a Ne matrix show more structure and are narrower than those of QTR in a water matrix. The 650 nm band of neutral QTR shown in Figure 1 has a FWHH of nearly 35 nm whereas the fwhh for the same transition in Ne at 608 nm is about 9 nm. Furthermore, the vibronic bands of QTR in a neon matrix show substructure that is not evident in the spectra in the ice matrix shown in Figure 1. At our resolution of 0.44 nm, the neon matrix substructure would be resolvable. The lack of such structure indicates that, in amorphous water ice, inhomogeneous line broadening due to sites is far more dominant than in neon matrices.

Although they did not report the double ionization of QTR to QTR^{2+} in a neon matrix, Halasinski et al. observed formation of the radical anion QTR^- via electron capture by neutral QTR.[25] Upon in-situ photolysis, these authors detected absorption by the radical cation (QTR^+) at 835 nm when matrices contained NO_2, an electron trap. In the absence of NO_2, absorption bands

attributed to both the radical cation and radical anion (QTR^-) were detected, the anion absorbing at longer wavelengths at 880 nm compared to the cation at 835 nm. This raises questions regarding the possibility of QTR^- formation in irradiated water ice. Though this cannot be ruled out on the basis of the experiments reported here, we do not observe any significant absorption at wavelengths longer than that of QTR^+ at 860 nm. However, it is possible that a very broad shoulder evident in the spectra shown in Figure 1 may indeed be due to the radical anion of quaterrylene. This feature which peaks near 910 nm appears to grow in continuously with photolysis and is clearly evident after 600 s of photolysis time.

In a water matrix, the absorption of doubly ionized quaterrylene, QTR^{2+}, occurs at a shorter wavelength (782 nm) than does the absorption of the quaterrylene monocation, QTR^+ (850 nm). Because no corresponding absorption is detected in a Ne matrix[25] we conclude that double ionization of QTR is not facilitated in a Ne matrix. This difference in behavior likely originates from the 2−3 eV electron affinity of a water matrix,[32,33] versus the negative electron affinity for a neon matrix of −1.3 eV.[34,35] In Ne matrices, electrons are not bound to the lattice. As a consequence, in Ne, electrons recombine efficiently with QTR^+ or are captured by neutral QTR molecules, generating the anion, QTR^-. Conversely, the electron is strongly solvated in water matrices and trapped locally by H_2O molecules, hindering its recombination with other QTR species.

Conclusions

The case has been made for the production and stabilization of QTR^{2+}, a closed shell dication, in a water matrix by the sequential photoionization: $QTR \rightarrow QTR^+ \rightarrow QTR^{2+}$. These findings, combined with recent experimental and theoretical results, show that ionization in water-ices is not unusual, but an important process. Cryogenic water matrices assist in-situ, stepwise, multiple photoionization processes and stabilize otherwise very reactive ionic products such as QTR^{2+} reported here. The electron affinity of water lowers the ionization energy of trapped species *and* stabilizes the ionized products. Lower ionization energies of QTR and QTR^+ in water-ice and the ability of the water matrix to stabilize both ionized species and generated electrons allows the significant single and double photoionization processes observed here with relatively mild photon energies ($\leq$10.2 eV) and fluxes. These findings are important for our understanding of the chemistry and physics of low-temperature water-rich ices that are abundant in our Solar System and also in the interstellar medium. The water-assisted lowering of organic molecule ionization energies may also play a role in terrestrial chemistry. For example, related water assisted process involving charged species could be important in the chemistry of stratospheric aerosols and ices containing anthropogenic impurities in the Polar Regions of the earth.[36]

Acknowledgment. This work was supported by grants from NASA's Exobiology, Astrobiology, and Long Term Space Astrophysics Programs (Grants: 344-58-12, 344-53-92, and 399-20-40 respectively), NASA's Planetary Geology and Geophysics Program (Grant: NNG05GI01G) and a NASA−University of Maryland cooperative agreement (NCC 2-1303). We thank the referees, whose reviews helped to improve this publication significantly.

References and Notes

(1) van Dishoeck, E. F. *Annu. Rev. Astron. Astrophys.* **2004**, *42*, 119.

(2) Cruikshank, D. P.; Brown, R. H.; Calvin, W. M.; Roush, T. L.; Bartholomew, M. J. Ices on the satellites of Jupiter, Saturn, and Uranus. In *Solar System Ices*; Schmitt, B., de Bergh, C., Festou, M., Eds.; Kluwer Academic Publishers: Dordrecht, Netherlands, 1998; p 576.

(3) Roush, T. L. *J. Geophys. Res.-Planets* **2001**, *106*, 33315.

(4) Prenni, A. J.; Tolbert, M. A. *Acc. Chem. Res.* **2001**, *34*, 545.

(5) Bernstein, M. P.; Sandford, S. A.; Allamandola, L. J.; Chang, S.; Scharberg, M. A. *Astrophys. J.* **1995**, *454*, 327.

(6) Bernstein, M. P.; Sandford, S. A.; Allamandola, L. J.; Gillette, J. S.; Clemett, S. J.; Zare, R. N. *Science* **1999**, *283*, 1135.

(7) Bernstein, M. P.; Dworkin, J. P.; Sandford, S. A.; Cooper, G. W.; Allamandola, L. J. *Nature* **2002**, *416*, 401.

(8) Gerakines, P. A.; Moore, M. H.; Hudson, R. L. *J. Geophys. Res.-Planets* **2001**, *106*, 33381.

(9) Gerakines, P. A.; Schutte, W. A.; Ehrenfreund, P. *Astron. Astrophys.* **1996**, *312*, 289.

(10) Muñoz Caro, G. M.; Meierhenrich, U. J.; Schutte, W. A.; Barbier, B.; Arcones Segovia, A.; Rosenbauer, H.; Thiemann, W. H.-P.; Brack, A.; Greenberg, J. M. *Nature* **2002**, *416*, 403.

(11) Gudipati, M. S.; Allamandola, L. J. *Astrophys. J. Lett.* **2003**, *596*, L195.

(12) Gudipati, M. S. *J. Phys. Chem. A* **2004**, *108*, 4412.

(13) Gudipati, M. S.; Allamandola, L. J. *Astrophys. J. Lett.* **2004**, *615*, L177.

(14) Woon, D. E.; Park, J.-Y. *Astrophys. J.* **2004**, *607*, 342.

(15) Crespo-Hernández, C. E.; Arce, R.; Ishikawa, Y.; Gorb, L.; Leszczynski, J.; Close, D. M. *J. Phys. Chem. A* **2004**, *108*, 6373.

(16) Gudipati, M. S.; Allamandola, L. J. *Astrophys. J.* **2006**, *638*, 286.

(17) Shafizadeh, N.; Sorgues, S.; Soep, B. *Chem. Phys. Lett.* **2004**, *391*, 380.

(18) Robson, L.; Ledingham, K. W. D.; Tasker, A. D.; McKenna, P.; McCanny, T.; Kosmidis, C.; Jaroszynski, D. A.; Jones, D. R.; Issac, R. C.; Jamieson, S. *Chem. Phys. Lett.* **2002**, *360*, 382.

(19) Rühl, E.; Price, S. D.; Leach, S. *J. Phys. Chem.* **1989**, *93*, 6312.

(20) Johnson, R. E.; Quickenden, T. I. *J. Geophys. Res.* **1997**, *102*, 10985.

(21) Sieger, M. T.; Simpson, W. C.; Orlando, T. M. *Naure* **1998**, *394*, 554.

(22) Klánová, J.; Klán, P.; Nosek, J.; Holoubek, I. *Environ. Sci. Technol.* **2003**, *37*, 1568.

(23) Herring-Captain, J.; Grieves, G. A.; Alexandrov, A.; Sieger, M. T.; Chen, H.; Orlando, T. M. *Phys. Rev. B* **2005**, *72*, 035431.

(24) Gudipati, M. S.; Dworkin, J. P.; Chillier, X. D. F.; Allamandola, L. J. *Astrophys. J.* **2003**, *583*, 514.

(25) Halasinski, T. M.; Weisman, J. L.; Ruiterkamp, R.; Lee, T. J.; Salama, F.; Head-Gordon, M. *J. Phys. Chem. A* **2003**, *107*, 3660.

(26) Kimmel, G. A.; Orlando, T. M. *Phys. Rev. Lett.* **1995**, *75*, 2606.

(27) Yabushita, A.; Hashikawa, Y.; Ikeda, A.; Kawasaki, M.; Tachikawa, H. *J. Chem. Phys.* **2004**, *120*, 5463.

(28) Jenniskens, P.; Blake, D. F. *Science* **1994**, *265*, 753.

(29) Frisch, M. J.; Trucks, G. W.; Schlegel, H. B.; Scuseria, G. E.; Robb, M. A.; Cheeseman, J. R.; Montgomery, J. A., Jr.; Vreven, T.; Kudin, K. N.; Burant, J. C.; Millam, J. M.; Iyengar, S. S.; Tomasi, J.; Barone, V.; Mennucci, B.; Cossi, M.; Scalmani, G.; Rega, N.; Petersson, G. A.; Nakatsuji, H.; Hada, M.; Ehara, M.; Toyota, K.; Fukuda, R.; Hasegawa, J.; Ishida, M.; Nakajima, T.; Honda, Y.; Kitao, O.; Nakai, H.; Klene, M.; Li, X.; Knox, J. E.; Hratchian, H. P.; Cross, J. B.; Adamo, C.; Jaramillo, J.; Gomperts, R.; Stratmann, R. E.; Yazyev, O.; Austin, A. J.; Cammi, R.; Pomelli, C.; Ochterski, J. W.; Ayala, P. Y.; Morokuma, K.; Voth, G. A.; Salvador, P.; Dannenberg, J. J.; Zakrzewski, V. G.; Dapprich, S.; Daniels, A. D.; Strain, M. C.; Farkas, O.; Malick, D. K.; Rabuck, A. D.; Raghavachari, K.; Foresman, J. B.; Ortiz, J. V.; Cui, Q.; Baboul, A. G.; Clifford, S.; Cioslowski, J.; Stefanov, B. B.; Liu, G.; Liashenko, A.; Piskorz, P.; Komaromi, I.; Martin, R. L.; Fox, D. J.; Keith, T.; Al-Laham, M. A.; Peng, C. Y.; Nanayakkara, A.; Challacombe, M.; Gill, P. M. W.; Johnson, B.; Chen, W.; Wong, M. W.; Gonzalez, C.; Pople, J. A. *Gaussian 03*, revision B.05; Gaussian Inc.: Pittsburgh, PA, 2003.

(30) Hirata, S.; Head-Gordon, M. *Chem. Phys. Lett.* **1999**, *302*, 375.

(31) Carl, E.; Schmidt, W. *Tetrahedron* **1978**, *34*, 3219.

(32) Novakovskaya, Y. V.; Stepanov, N. F. *Struct. Chem.* **2004**, *15*, 65.

(33) Khan, A. *J. Chem. Phys.* **2004**, *121*, 280.

(34) Song, K. S.; Williams, R. T. In *Self-Trapped Excitons*; Cardona, M., Ed.; Springer: Berlin, 1996; Vol. 103.

(35) Frankowskia, M.; Savchenko, E. V.; Smith-Gicklhorn, A. M.; Grigorashchenko, O. N.; Gumenchuk, G. B.; Bondybey, V. E. *J. Chem. Phys.* **2004**, *121*, 1474.

(36) Klán, P.; Holoubek, I. *Chemosphere* **2002**, *46*, 1201.